Two-stage Spinel Growth in the High-Grade Metapelites of the Central Kerala Khondalite Belt: Implication for Prograde P–T path

K.P. SHABEER[1], K. SAJEEV[2], T. OKUDAIRA[1] and M. SANTOSH[3]

1) Department of Geosciences, Faculty of Science, Osaka City University, Osaka 558-8585, Japan

2) Department of Earth Sciences, Okayama University, Okayama 700-8530, Japan

3) Department of Natural Environmental Science, Kochi University, Kochi 780-8520, Japan

Abstract

Two generations of spinels are identified from the granulite facies metapelites of the central Kerala Khondalite Belt, southern India. Spinels of the first generation show brownish color and were formed during prograde metamorphism by the consumption of Zn-, Cr- bearing biotite, together with garnet and sillimanite following the prograde reaction: Bt + Grt + Sil = Spl + Crd + Kfs + Melt. The formation of second-generation greenish spinels occurred during a subsequent retrograde stage following the reaction: Grt + Sil = Spl + Crd + Qtz. The textural features indicate a close association of the first generation brown spinels and biotite. Biotite contains up to 0.34 wt% of ZnO and 0.30 wt% of Cr_2O_3. Individual grains of brownish spinel show a continuous compositional zoning owing to increasing Zn and Cr contents towards the grain margins. These chemical and textural observations suggest that the brown spinels formed by the breakdown of Zn and Cr-rich biotite. It is proposed that the zinc-saturation limit of biotite depends on the metamorphic conditions, and that decreasing pressure with increasing temperature led to the release of Zn from biotites resulting in the formation of brownish spinels.

Key-words : Kerala Khondalite Belt, high grade metapelite, spinel, biotite, zinc saturation

1. Introduction

Spinel with compositions intermediate between hercynite and gahnite are common in high to medium grade metapelites having garnet-biotite-cordierite-sillimanite as stable assemblage. The origin of the spinels in the series (Fe, Mg, Zn) Al_2O_4 has commonly been ascribed to high-temperature/low-pressure metamorphism of silica-poor rocks, or to zinc ore bodies or pegamatites enriched in Zn (e.g., Rumble, 1976). Spinel is less commonly observed in low-grade rocks, where their formation is attributed to the breakdown of staurolite (Robinson and Jaffe, 1969; Loomis, 1972; Stoddard, 1979) or sphalerite (Plimer, 1977; Wall and England, 1979). Furthermore, the formation of spinel is also aided by the breakdown of zinc bearing biotites during decompression process (Dietvorst, 1980). In this paper, we discuss the crystallization process of Fe-rich, Cr and Zn-bearing spinels and the inferred P-T path of the high-grade supracrustals of Kerala Khondalite Belt, southern India.

2. Regional Framework

The Kerala Khondalite Belt (KKB) constitutes vast supracrustal rocks of granulite grade, bounded on the north by the Achankovil Shear Zone and in the south by the Nagercoil Granulite Block (Chacko et al., 1987, Santosh, 1996). Evidence for multiple metamorphic events culminating in granulite facies metamorphism and extensive crustal rejuvenation during late Pan-African event of ca. 540 Ma has been documented from this area (Harris et al., 1994; Fonarev et al., 2000). The

major lithologies in this belt include garnet-bearing charnockites, garnet + biotite + sillimanite + cordierite + K-feldspar + quartz ± spinel gneisses (khondalites), garnet-biotite-quartz-feldspar gneisses (leptynites), minor two pyroxene granulites and calc-silicate rocks. Charnockites dominate towards the northern and southern margins, while the central part of KKB mostly comprises spinel-bearing khondalites and leptynites.

KKB has attracted much attention in the past for its spectacular preservation of "arrested charnockite" structures in quarry section, where garnet- and biotite-bearing upper amphibolite facies gneisses show prograde transformation to patches, veins and lenses of orthopyroxene-bearing "incipient charnockites" (Ravindra Kumar and Chacko, 1986; Srikantappa et al., 1985; Hensen, 1987; Raith et al., 1989; Santosh et al., 1990). The gneiss-charnockite transformation is often structurally controlled, and has been correlated to the influx of CO_2-rich fluids, which buffered the water activity, thereby stabilizing the orthopyroxene in charnockite (Hansen et al., 1987, Santosh et al., 1990).

Due to the widespread exposures and the varied processes preserved, the KKB has been one of the intensely studied granulite terrains among the East Gondwana fragments. However, the metamorphic history of the KKB supracrustals has remained elusive despite previous studies, and the peak metamorphic pressure-temperature (P-T) conditions and exhumation history of the belt have been a topic of debate. Pressure-temperature estimates of the KKB rocks in the previous studies are largely based on conventional geothermobarometry, relying mainly on Fe-Mg exchange between coexisting minerals. These computations yielded moderate P-T conditions in the range of 600-750℃ and 4-5Kbar (Chacko et al., 1987; Hansen et al., 1987). More recent studies (e.g., Chacko et al., 1996; Satish-Kumar and Harley, 1998; Nandakumar and Harley, 2000) revealed higher temperatures in the range of >830℃ and even >900℃, based on mineral phase equilibria in calc-silicate rocks interlayered with the pelitic and semi-pelitic lithologies, and peak temperatures of 900 ± 20℃ at pressure of 6.5-7 kbar were suggested for the rocks from the northeastern and southern extremities of the belt. Braun et al. (1996) suggested
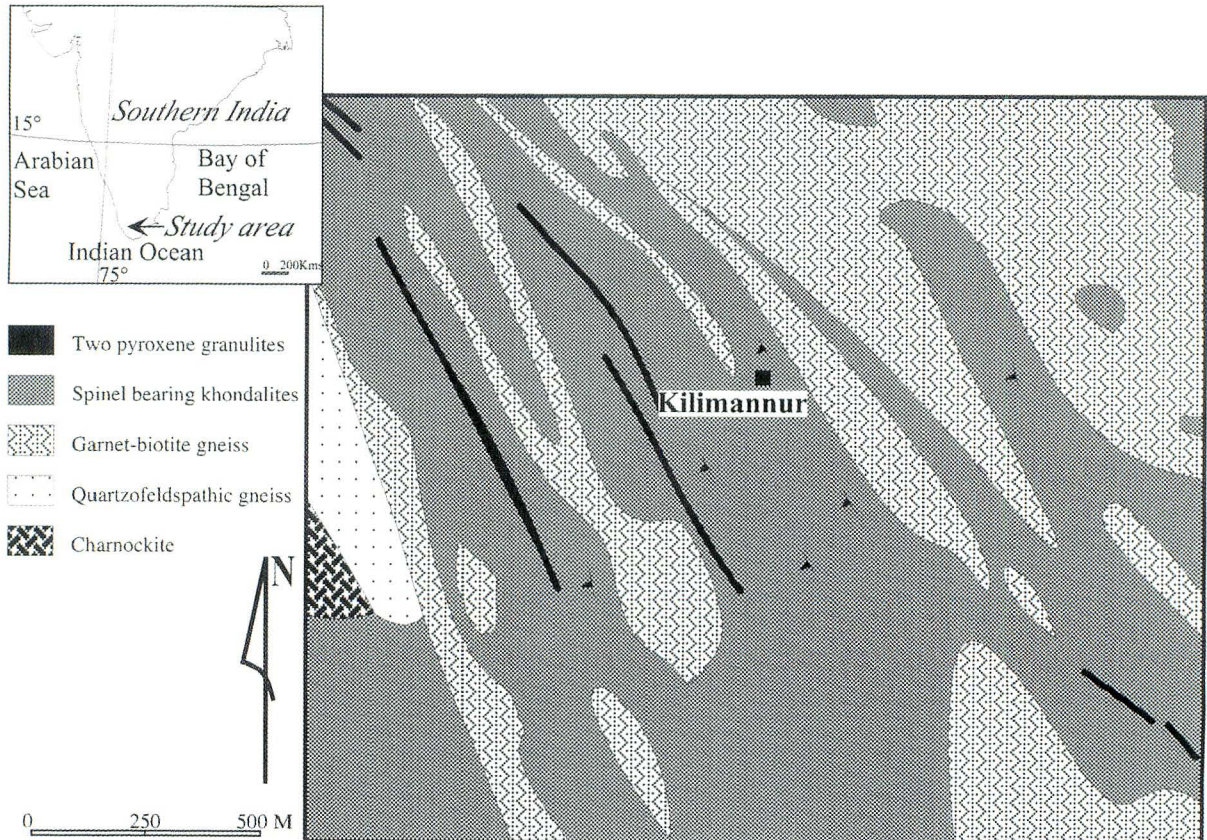

Fig. 1   Geological map of the study area showing the lithological units (modified after Geological Survey of India, 1995).

the occurrence of migmatitic gneisses and garnet-bearing leucogneisses as evidence for melting reactions under fluid absent conditions during peak temperature.

3. Field Geology

The present study was carried out in the central part of KKB around Kilimanur area, about 40 km north of Trivandrum city, were metasupracrustals are exposed in a chain of hillocks with numerous active quarries. A geological map of the study area is shown in Fig. 1.

The metapelites with the assemblage of cordierite + garnet + sillimanite + spinel + biotite + quartz + plagioclase + K-feldspar are very well exposed in this area (Fig. 2a). These gneisses show effects of multiple deformation and migmatisation. Migmatisation resulting in the formation of partially discordant leucosomes are commonly seen in all the areas. These migmatites with stromatic structure extend over several kilometers in the central KKB. Layers of cordierite-garnet-biotite-sillimanite-spinel assemblage alternating with quartzo-feldspathic layers define the compositional lay-

Fig. 2 (a) Field photograph of a migmatite quarry in Kilimanur, (b) A closer view of spinel bearing gneissic band from the study area. Layered quartz bearing migmatite with the spinel-cordierite bearing leucosome can be clearly seen.

ering in the rock (Fig. 2b). In some places, elongate khondalite lenses are boudinaged by enclosing leucosomes.

The granitic layers are composed of coarse anhedral crystals of quartz and feldspar. These layers commonly contain small reddish garnet. The melanosome is a relatively silica poor assemblage comprised of cordierite, spinel, garnet, sillimanite, biotite and oxide phases. Cordierite occurs both in the layers and as large discrete grains. In some domains, cordierite occurs around corroded garnet grains. In some of the exposures, tiny disseminated flakes of graphite are also seen. Quartz veins with scheelite crystals were recently reported from within the gneisses of this area (Shabeer et al., 2001). Orthopyroxene-bearing zones of incipient charnockites were not found in these locations, probably due to the highly aluminous bulk chemistry of the metapelites, which inhibits the formation of orthopyroxene. However, arrested charnockite formation is noticed in some of the garnet-biotite gneisses, of which the aluminous minerals such as sillimanite and spinel are absent.

The compositional layering constitutes the main planar structure. The general trend of the compositional layering, which is confirmable in all the exposures of the area, is generally N50°W-S50°E dipping towards east. The deformational events, which developed the regional foliation (D1) synchronous with high-grade metamorphism and the subsequent deformation (D2) resulting in the formation of a series of upright folds, are preserved in these rocks.

The samples of the present study were all collected from the fresh active quarries. The wide distribution of active quarries with accessible roads in this area provided good opportunity for sampling a large tract of the supracrustals of the central KKB.

4. Petrography and Mineral Chemistry

Petrographic studies were carried out in a number of thin sections using a polarizing microscope and the chemistry of the constituent minerals was determined using an electron-probe microanalyzer (Shimadzu, EPMA-8705) at Osaka City University, Japan. For the chemical analyses, an accelerating voltage of 15 kV, beam current of 4 nA and a beam diameter of 1 μm were used. Data acquisition and reduction were performed using the method of Bence and Albee (1968). Natural and synthetic oxides and silicate minerals were used as standards. The representative analyses of major mineral phases are given in Tables 1, 2 and 3. The tex-

tural features and the chemistry of the major mineral phases are briefly summarized in the following sections.

The dominant minerals in the metapelites are garnet, biotite, cordierite, K-feldspar, spinel, sillimanite and quartz, with minor plagioclase. The accessories include zircon and opaque phases. A petrographic sketch showing a typical metapelite assemblage from the central KKB is shown in Fig. 3. Spinel is a common accessory mineral in all the samples studied here. Petrographic study coupled with EPMA data reveals the presence of two distinct generations of spinels in the study area. Two types of spinels that have been recognized are greenish variety and a brownish variety. The green spinels occur as porphyroblasts, and these spinels are generally associated with cordierite (Fig. 4a, a'). Some small-grained greenish spinels are seen as inclusion in garnet. The brownish spinels are newly
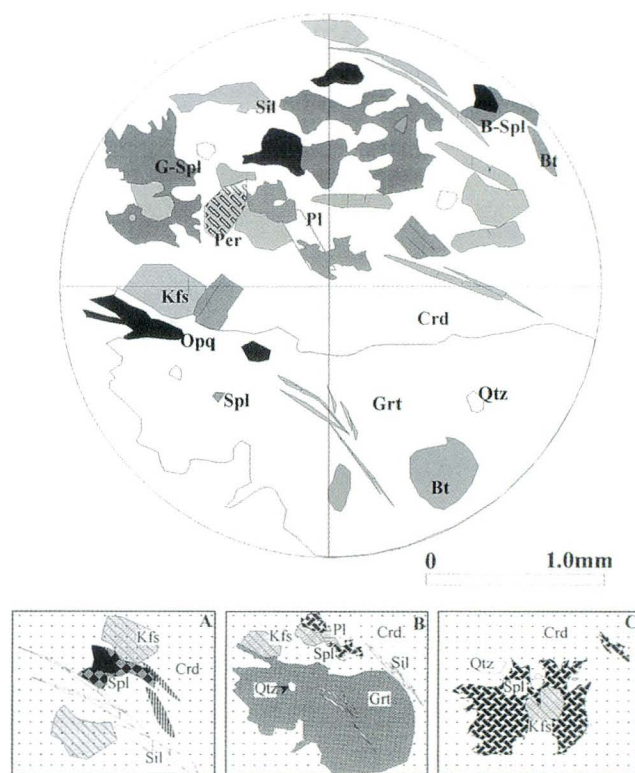

Fig. 3   Petrographic sketch representing the mineral assemblage and their microtextural relationships in the spinel-bearing metapelite of the study area:
A. brownish spinel grain formed in association with cordierite and K-feldspar seen in the proximity of sillimanite, B. spinel and cordierite replacing garnet and sillimanite in the low strain zone, C. a late corona of cordierite separating spinel and quartz from direct contact.
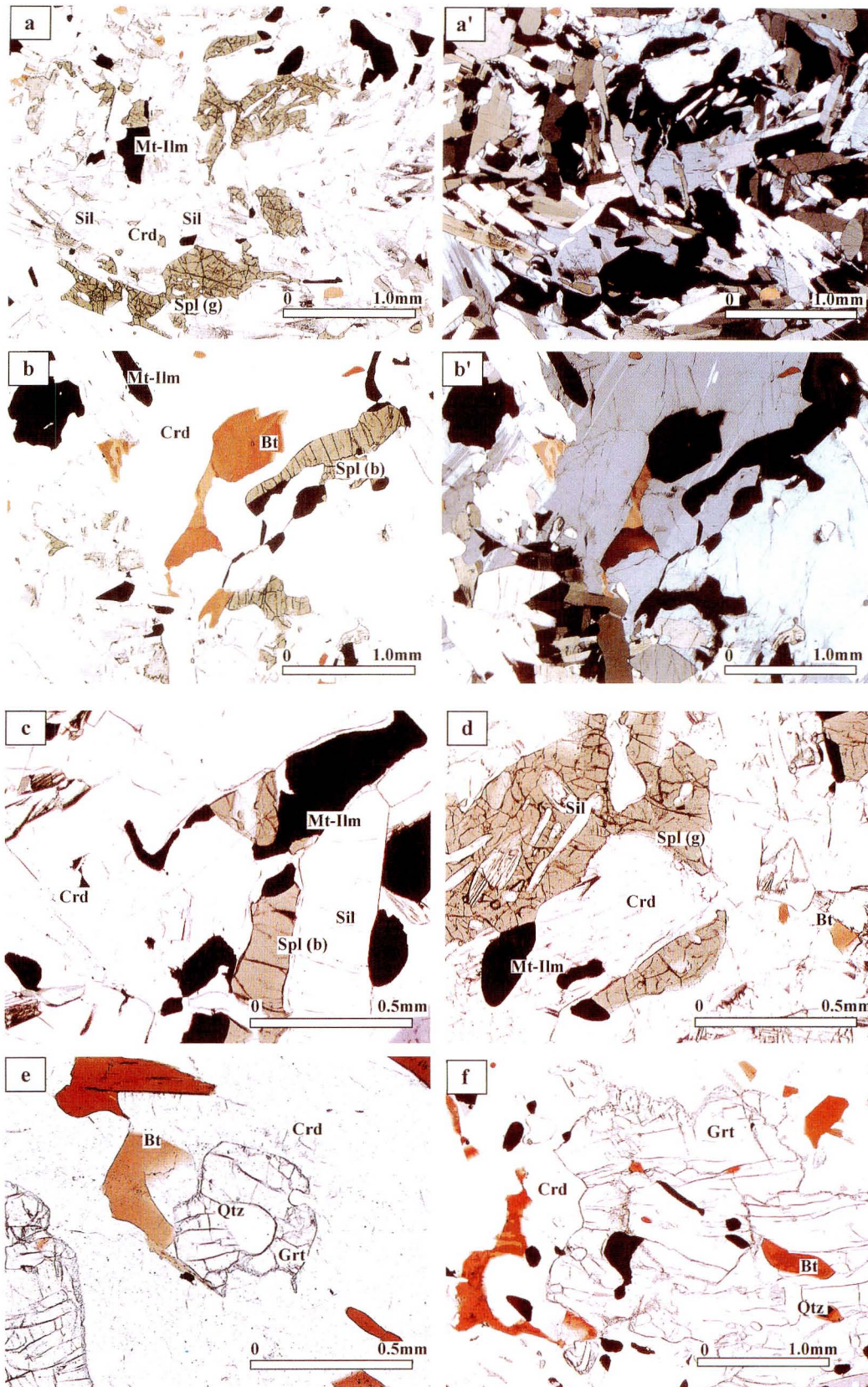
Fig. 4   (a) Photomicrograph showing the greenish spinel in association with cordierite and sillimanite. Note that biotite is almost absent in this domain, (a'): view of the same assemblage under crossed nicols, (b) brownish spinel formed in the proximity of biotite, (b') same assemblage under crossed nicols, (c) brownish spinel close to a sillimanite grain, (d) greenish spinel carrying inclusions of sillimanite (e) cordierite corona formed around garnet (f) a garnet porphyroblast with numerous inclusions of biotite, quartz and oxide phases.
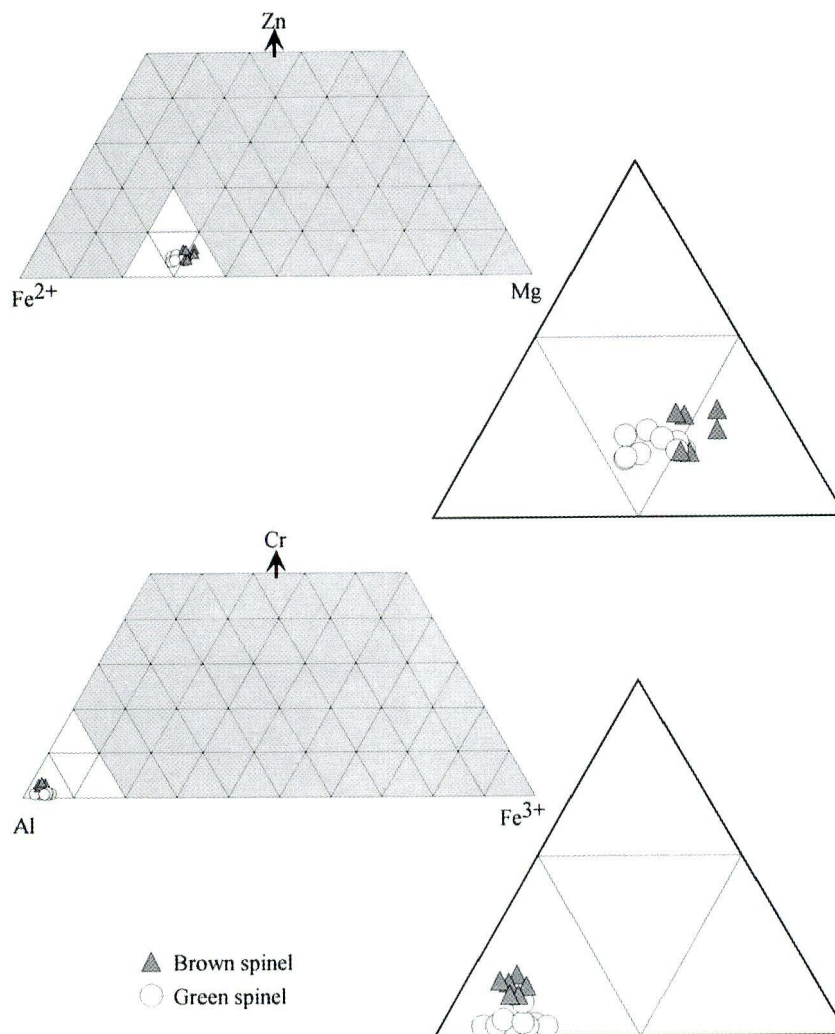
Fig. 5   Spinel composition represented in $Zn-Fe^{2+}-Mg$ and $Cr-Al-Fe^{3+}$ diagrams showing the variation in compositions of green and brown spinels.

identified in this study, which are seen as brown colored grains with an approximate size of >5 mm, often associated with biotite or carrying inclusions of biotite (Fig. 4b, b' and c). Mineral chemistry also clearly distinguishes two spinel varieties, as will be discussed in a later section. The two varieties of spinels are distributed along with polygonal grains of feldspar and cordierite in a fine-grained matrix of biotite. The major inclusions found in spinels are biotite, cordierite and feldspar. Inclusions of fibrolite are also found in some of the spinels (Fig. 4d).

The brown spinels are distributed in the close proximity of biotite. Appreciable content of zinc (Zn = 2.6 - 3.30 wt%) and chromium is noticed in these spinels. Each spinel grain shows a tendency towards more Zn- and Cr- rich compositions with increasing proximity towards biotite. The spinels found in the close vicinity of biotites are more zinician than those away from

biotite grains. Besides spinel, biotite is the only mineral phase that carries Zn and Cr among the mineral assemblage in these rocks. The brownish color of these spinels is attributed to the appreciable content of Cr_2O_3 (2.4 - 3 wt%), (Fig. 5). Minor amount of Ti is also present in this variety (TiO_2 ranging from 0.2 - 0.4 wt%). Both spinels show compositional zoning, with increase in zinc content towards the edge of the grain (see Table 1). The Mg and Fe content of all the spinels are almost consistent with not much variation. As a consequence, the spinel $Fe^{2+}/(Fe^{2+}+Mg)$ ratio is not systematically correlated with the substitution of Zn.

The greenish variety of spinels in association with cordierites or forming intergrowth texture is mainly concentrated in the proximity of garnets, and the cordierites commonly separate spinel from garnet. The chemical analyses of these spinels show comparatively less zinc content 1.30 - 1.90 wt%. Complete absence of chromium

Table 1   Compositional variation in the two generations of spinel from KKB.
('B' represents the compositions of brownish spinel and 'G' corresponds to the greenish variety).

	Spinel Composition										
Anal. No.	**B** Tvm7	**B** Tvm8	**B** Tvm9	**B** Tvm10	**B** Tvm11	**G** Tvm14	**G** Tvm26	**G** Tvm28	**G** Tvm29	**G** Tvm30	**G** Tvm6
SiO₂	0.00	0.00	0.00	0.00	0.00	0.00	0.00	0.00	0.00	0.00	0.00
TiO₂	0.30	0.30	0.20	0.30	0.40	0.20	0.10	0.00	0.10	0.30	0.00
Al₂O₃	56.30	56.20	57.30	56.30	56.60	57.10	58.10	56.70	57.00	58.60	57.70
Cr₂O₃	2.80	2.50	2.30	3.00	2.40	0.60	1.00	0.00	0.80	0.00	0.90
FeO	31.30	31.30	31.20	30.70	31.00	33.20	32.20	33.30	33.60	32.40	32.10
MnO	0.00	0.00	0.00	0.00	0.00	0.00	0.00	0.00	0.00	0.00	0.00
MgO	6.60	6.60	6.40	7.00	7.00	7.40	7.10	7.80	7.30	7.40	7.40
CaO	0.10	0.10	0.00	0.00	0.20	0.00	0.10	0.00	0.00	0.00	0.00
Na₂O	0.00	0.40	0.00	0.00	0.00	0.00	0.00	0.00	0.00	0.00	0.10
K₂O	0.00	0.00	0.00	0.00	0.00	0.00	0.00	0.30	0.00	0.00	0.00
ZnO	3.30	3.20	3.00	3.00	2.60	1.50	1.30	1.50	1.20	1.30	1.90
Total	**100.70**	**100.60**	**100.40**	**100.30**	**100.20**	**100.00**	**99.90**	**99.60**	**100.00**	**100.00**	**100.10**
O	4	4	4	4	4	4	4	4	4	4	4
Si	0.000	0.000	0.000	0.000	0.000	0.000	0.000	0.000	0.000	0.000	0.000
Ti	0.006	0.006	0.004	0.006	0.008	0.004	0.002	0.000	0.002	0.006	0.000
Al	1.871	1.871	1.900	1.871	1.879	1.898	1.920	1.896	1.896	1.930	1.910
Cr	0.062	0.056	0.051	0.067	0.053	0.013	0.022	0.000	0.018	0.000	0.020
Fe	0.738	0.739	0.734	0.724	0.730	0.783	0.755	0.790	0.793	0.757	0.754
Mn	0.000	0.000	0.000	0.000	0.000	0.000	0.000	0.000	0.000	0.000	0.000
Mg	0.277	0.278	0.268	0.294	0.294	0.311	0.297	0.330	0.307	0.308	0.310
Ca	0.003	0.003	0.000	0.000	0.006	0.000	0.003	0.000	0.000	0.000	0.000
Na	0.000	0.022	0.000	0.000	0.000	0.000	0.000	0.000	0.000	0.000	0.005
K	0.000	0.000	0.000	0.000	0.000	0.000	0.000	0.011	0.000	0.000	0.000
Zn	0.069	0.067	0.062	0.062	0.054	0.031	0.027	0.031	0.025	0.027	0.039
Total cation	2.958	2.975	2.958	2.962	2.971	3.009	3.000	3.026	3.016	3.002	2.999
Fe³⁺	0.060	0.067	0.045	0.056	0.059	0.085	0.055	0.104	0.084	0.064	0.070
Fe²⁺	0.678	0.672	0.690	0.668	0.671	0.698	0.700	0.686	0.709	0.694	0.683
Fe³⁺/Fe²⁺	0.089	0.100	0.065	0.083	0.088	0.121	0.079	0.152	0.119	0.092	0.103
XMg*	0.290	0.292	0.280	0.306	0.304	0.308	0.298	0.325	0.302	0.308	0.312
XMg	0.273	0.273	0.268	0.289	0.287	0.284	0.282	0.294	0.279	0.289	0.291

is noticed in these varieties in contrast to the brownish spinels. Spinel in some of the domains exists very close to quartz grains, although spinel grains are not in direct contact with quartz, and the two phases are separated by thin lamella of cordierite.

Biotite grains are seen both as inclusions in garnet and spinel and as matrix grains. Zinc and chromium are minor elements in biotite that co-exists with spinel in these rocks. The content of these elements varies with distance from the brown spinel. It is seen that the biotite grains close to the brownish spinels contain 0.04 wt% of ZnO and that the zinc content of biotite increases gradually up to 0.34 wt% at distance exceeding 2 mm from the grain contact. The chromium content also shows the same feature with Cr_2O_3 ranging from 0 to 0.30 wt%. High fluorine content noticed in these biotites (F = 0.55-0.78) indicates their high temperature stability (Carigton and Harley, 1995 and Hensen and Osanai, 1994). The TiO_2 content in the biotites ranges between 4.90-7.20 wt%.

Cordierites occur as porphyroblasts or clusters of subhedral grains forming the matrix. Cordierite also forms symplectitic "finger-print" like intergrowth with quartz, biotite and K-feldspar. The subhedral grains display a texturally equilibrated mosaic of polygonal grains of 3 mm to 5 mm in size, exhibiting the characteristic sector-twin. These grains carry inclusions of sillimanite, greenish spinel, biotite, K-feldspar and minor amount of zircon. Subhedral cordierite grains are mostly concentrated near to the rim of garnet (Fig. 4e). Based on the microstructure, the cordierites in these rocks can be classified in to two categories; 1) cordierite associated with brownish spinel, and 2) cordierite in association with greenish spinel or cordierite that forms symplectites. Although the X_{Mg} value does not show much variation among these categories, the total oxide weight percentage in probe analyses vary considerably, probably reflecting the role of volatiles.

Garnet porphyroblasts are frequently present with grain size approximately >6 mm and exhibiting sieve

Table 2　Composition of biotites.

Anal. No.	Tvm2	Tvm13	Tvm16	Tvm24	Tvm 19	Tvm18	Tvm15	Tvm2b	Tvm12
Biotite Composition									
SiO_2	36.10	36.20	36.30	36.90	37.19	37.20	37.30	37.00	35.50
TiO_2	6.30	5.40	7.20	4.90	5.50	5.50	5.10	5.10	5.80
Al_2O_3	14.50	14.60	14.80	15.50	14.19	14.20	15.10	14.10	14.10
Cr_2O_3	0.00	0.00	0.10	0.15	0.20	0.22	0.25	0.30	0.32
FeO	14.80	17.50	16.30	15.40	15.15	15.10	14.70	13.90	18.90
MnO	0.00	0.00	0.00	0.00	0.00	0.00	0.00	0.00	0.00
MgO	13.60	11.50	11.00	13.20	12.65	12.70	13.20	14.90	10.60
CaO	0.00	0.20	0.00	0.40	0.13	0.10	0.00	0.10	0.00
Na_2O	0.30	0.30	0.40	0.30	0.23	0.20	0.00	0.10	0.10
K_2O	10.10	10.30	10.00	9.10	10.72	10.70	10.40	10.30	9.50
ZnO	0.00	0.00	0.00	0.00	0.00	0.00	0.04	0.22	0.34
F	1.38	1.47	1.15	1.46	1.55	1.56	1.34	1.66	1.63
Cl	1.24	1.47	1.27	0.76	1.12	0.77	1.28	1.01	1.43
F=O	0.58	0.62	0.48	0.62	0.65	0.66	0.56	0.70	0.69
Cl=O	0.28	0.33	0.29	0.17	0.25	0.17	0.29	0.23	0.32
Total	97.46	97.99	97.75	97.28	97.72	97.42	97.86	97.76	97.21
H2O*	3.03	2.89	3.13	3.14	2.98	3.06	3.07	2.98	2.76
Total*	**100.49**	**100.88**	**100.87**	**100.43**	**100.70**	**100.48**	**100.93**	**100.75**	**99.97**
Si	5.414	5.485	5.451	5.492	5.577	5.578	5.549	5.510	5.460
Ti	0.711	0.615	0.813	0.548	0.620	0.620	0.571	0.571	0.671
Al	2.563	2.607	2.619	2.718	2.508	2.509	2.647	2.475	2.556
Cr	0.000	0.000	0.012	0.018	0.024	0.026	0.029	0.035	0.039
Fe	1.856	2.217	2.047	1.916	1.900	1.893	1.828	1.731	2.431
Mn	0.000	0.000	0.000	0.000	0.000	0.000	0.000	0.000	0.000
Mg	3.041	2.598	2.463	2.929	2.828	2.839	2.927	3.308	2.430
Ca	0.000	0.032	0.000	0.064	0.021	0.016	0.000	0.016	0.000
Na	0.087	0.088	0.116	0.087	0.067	0.058	0.000	0.029	0.030
K	1.932	1.991	1.915	1.727	2.051	2.047	1.973	1.957	1.864
Zn	0.000	0.000	0.000	0.000	0.000	0.000	0.004	0.024	0.039
O	22.000	22.000	22.000	22.000	22.000	22.000	22.000	22.000	22.000
F	0.654	0.704	0.546	0.687	0.735	0.740	0.630	0.782	0.793
Cl	0.315	0.378	0.323	0.192	0.285	0.196	0.323	0.255	0.373
OH	3.030	2.918	3.131	3.121	2.980	3.065	3.047	2.963	2.835
XMg^*	1.000	1.000	1.000	1.000	1.000	1.000	1.000	1.000	1.000
XMg	0.621	0.540	0.546	0.604	0.598	0.600	0.616	0.656	0.500
XFe	0.379	0.460	0.454	0.396	0.402	0.400	0.384	0.344	0.500
F/F+OH	0.164	0.176	0.137	0.172	0.184	0.185	0.158	0.195	0.198

texture with abundant mineral inclusions of biotite, swarms of sillimanite, K-feldspar, quartz and opaque phases (Fig. 4f). The garnet porphyroblasts in some portions contain rare, isolated and rounded inclusions of spinel, X_{Mg} of which is slightly higher than other discrete grains of spinels. Although we examined several thin sections, no traces of inclusions of kyanite or staurolite were found. Garnets also form coronal rinds around cordierite and greenish spinel. All the garnets show almandine-pyrope composition with a minor amount of grossular and spessartine with a rim-ward zonation (Alm_{66-70}, Pyr_{28-32}, Grs_{1-3}). The values of X_{Mg} range between 0.283-0.326; recalculation of X_{Mg} after deducting Fe^{3+} from Fe^{total} also shows same values of X_{Mg} indicating no pronounced oxidation effects.

Sillimanite occurs as rhombs or needles either as inclusions in garnet and cordierite, or as coarse and discrete idiomorphic grains, often close to garnet grains. Additionally, stringers of sillimanite are also seen dispersed near the brownish spinel. Occurrence of sillimanite grains is very heterogeneous. Analyses of the sillimanites indicate that all these have a near pure composition.

K-feldspar is a major phase present in the matrix and orthoclase content is about 88%. It is often perthitic, with thin stringers and blebs of exsolved sodic plagioclase. Discrete inclusions of plagioclase occur in subordinate amounts. Plagioclase occurs only as a subordinate phase in the studied metapelites, with albite-rich composition and lacking any appreciable zoning (An_{25-23}).

Most of the opaque phases show ilmenite compo-

Table 3   Analyses of cordierites and garnets.

Anal. No.	Garnet Composition				Cordierite Composition				
	Tvm21	Tvm25	Tvm27	Tvm 18	Tvm3	Tvm4	Tvm5	Tvm23	Tvm17
SiO$_2$	40.30	39.10	38.70	38.69	50.70	50.60	49.90	50.40	48.80
TiO$_2$	0.00	0.10	0.00	0.07	0.00	0.00	0.00	0.10	0.10
Al$_2$O$_3$	21.10	21.20	21.20	21.01	31.90	31.90	31.40	31.80	31.60
Cr$_2$O$_3$	0.00	0.20	0.00	0.00	0.20	0.00	0.00	0.00	0.30
FeO	29.80	31.24	32.20	32.40	5.50	5.60	6.60	5.50	7.10
MnO	0.00	0.00	0.00	0.00	0.00	0.00	0.40	0.00	0.30
MgO	8.10	7.30	7.20	7.16	10.00	10.00	9.90	10.40	9.80
CaO	0.80	1.20	0.70	0.75	0.00	0.10	0.10	0.00	0.00
Na$_2$O	0.10	0.10	0.00	0.00	0.10	0.20	0.20	0.00	0.00
K$_2$O	0.00	0.00	0.10	0.05	0.00	0.00	0.00	0.00	0.00
ZnO	0.00	0.00	0.00	0.00	0.00	0.00	0.00	0.00	0.00
Total	100.20	100.44	100.10	100.13	98.40	98.40	98.50	98.20	98.00
O	12	12	12	12	18	18	18	18	18
Si	3.103	3.038	3.028	3.030	5.137	5.132	5.097	5.118	5.026
Ti	0.000	0.006	0.000	0.004	0.000	0.000	0.000	0.008	0.008
Al	1.915	1.941	1.955	1.939	3.810	3.813	3.780	3.806	3.836
Cr	0.000	0.012	0.000	0.000	0.016	0.000	0.000	0.000	0.024
Fe	1.919	2.030	2.107	2.122	0.466	0.475	0.564	0.467	0.612
Mn	0.000	0.000	0.000	0.000	0.000	0.000	0.035	0.000	0.026
Mg	0.929	0.845	0.840	0.836	1.510	1.511	1.507	1.574	1.504
Ca	0.066	0.100	0.059	0.063	0.000	0.011	0.011	0.000	0.000
Na	0.015	0.015	0.000	0.000	0.020	0.039	0.040	0.000	0.000
K	0.000	0.000	0.010	0.005	0.000	0.000	0.000	0.000	0.000
Zn	0.000	0.000	0.000	0.000	0.000	0.000	0.000	0.000	0.000
Total cation	7.947	7.987	7.999	7.999	10.959	10.981	11.033	10.972	11.036
Fe3+	0.000	0.003	0.016	0.027	0.053	0.055	0.123	0.084	0.146
Fe2+	1.919	2.027	2.091	2.095	0.414	0.420	0.441	0.383	0.466
Fe3+/Fe2+	0.000	0.001	0.008	0.013	0.127	0.131	0.279	0.220	0.313
Alm	0.658	0.682	0.699	0.700	-	-	-	-	-
Spe	0.000	0.000	0.000	0.000	-	-	-	-	-
Pyr	0.319	0.284	0.281	0.279	-	-	-	-	-
Grs	0.023	0.030	0.014	0.012	-	-	-	-	-
Adr	0.000	0.004	0.006	0.009	-	-	-	-	-
XMg*	0.326	0.294	0.287	0.285	0.785	0.783	0.774	0.804	0.764
XMg	0.326	0.294	0.285	0.283	0.764	0.761	0.728	0.771	0.711

sition in ilmenite-hematite solid solution with thin lamella of magnetite. The Fe^{3+}/Fe^{2+} ratio varies from 1-1.1, suggesting moderate oxidation.

5. Metamorphic Reactions

The reaction textures observed in the metapelites indicate some prograde as well as retrograde reactions. Compositional relationship between the brown spinel and biotite suggests close association of the two phases, revealing that the breakdown of Zn- and Cr-bearing biotite produced Zn- and Cr-rich brownish spinels. Matrix-forming cordierite grains that coexist with brown spinel, in some places carry inclusions of garnet, biotite, sillimanite. This represents that cordierite and brown spinel are the reaction products derived from breakdown of garnet + biotite + sillimanite. These observations suggest the following reaction:

$$Bt + Grt + Sil = Spl + Crd + Kfs + liquid \qquad (1)$$
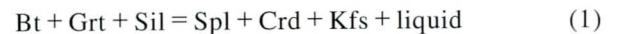
On considering the steep positive slope of the reaction in the P-T space (Fitzsimons, 1996), the assemblage in the right-hand side of the reaction is stable at higher temperature. Thus the formation of brownish spinels is considered to have occurred prior to the peak temperature and thereby, the reaction suggests a prograde P-T path of the metapelites.

The main retrograde reaction texture preserved is the symplectitic intergrowth of cordierite and greenish spinel along with quartz observed in the grain boundaries between garnet and sillimanite, which could represent the following reaction:
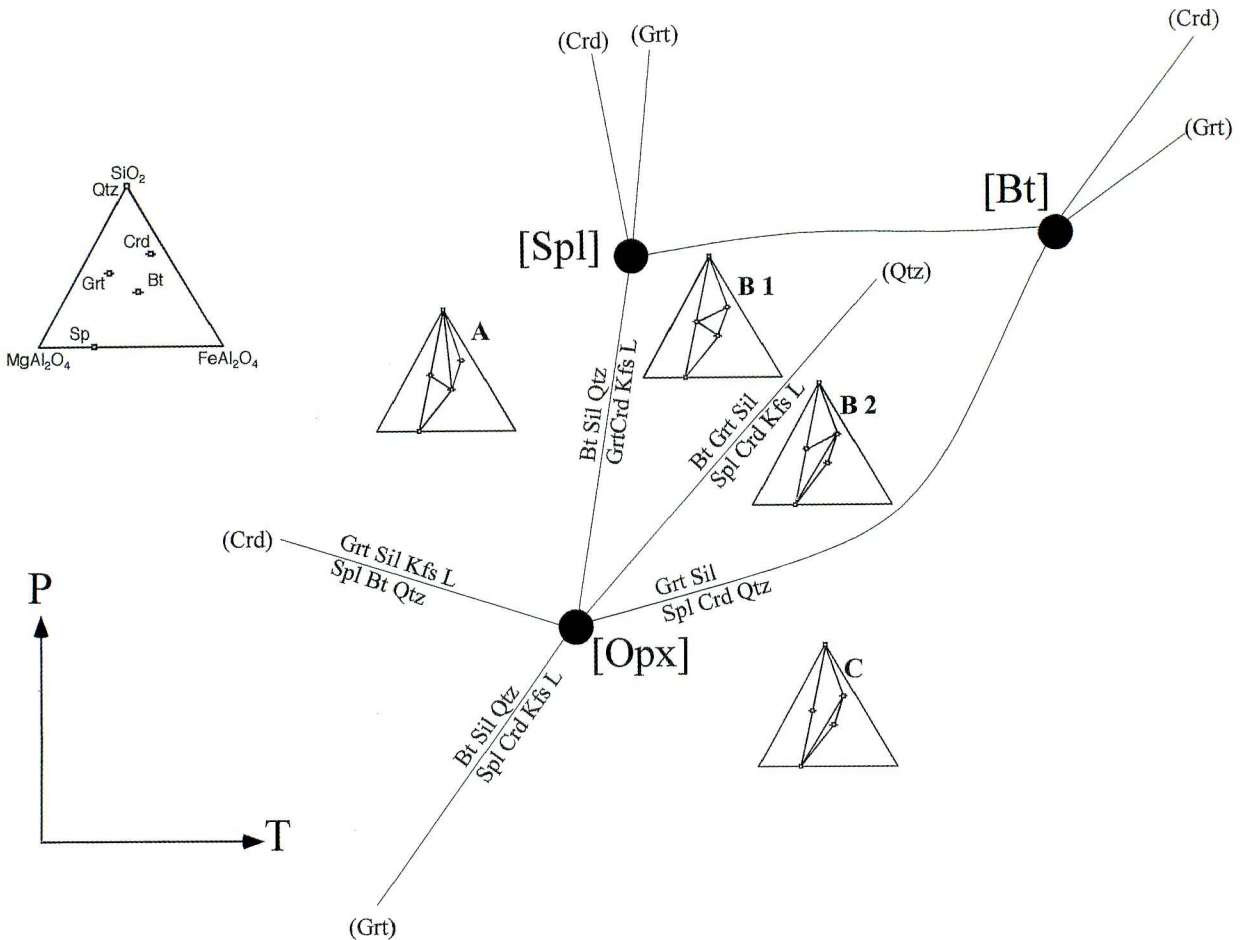
$$Grt + Sil = Spl + Crd + Qtz \qquad (2)$$

Fig. 6   A quantitative partial grid of KFMASH univariant reactions in P-T space for the observed mineral paragenesis (modified after Fitszimons, 1996). The reactions around [Opx] invariant point in the grid are divided in to the regions A, B 1, B 2 and C that corresponds to the stability fields of the different generation of the mineral assemblages. The KFMASH phase relationships projected in the SiO_2-$FeAl_2O_4$-$MgAl_2O_4$ plane is also illustrated with triplots in the petrogenetic grid.

The reaction (2) has a gentle slope and the right-hand assemblage in this reaction is stable at lower pressure. Therefore, the reaction suggests a decompressional P-T trajectory, similar to many granulite terrains (e.g., Harley et al., 1990; Fitzsimons, 1996).

According to the petrogenetic grid of Fitzsimons (1996), the reactions (1) and (2) are found around the orthopyroxene invariant point ([Opx] in Fig. 6) in the system of K_2O-FeO-MgO-Al_2O_3-SiO_2-H_2O (KFMASH). In this figure, mineral paragenesis of each stability field separated by reaction curves is also shown. The stability fields of B1 and B2 are dissected by reaction (1) for silica-poor metapelites. The involvement of the reaction (1) and reduced amount of quartz in the metapelites studied here may suggest silica-poor restitic character for the metapelites.

6. Pressure-Temperature Estimation

Fe-Mg cation exchange between coexisting garnet-cordierite and cordierite- spinel data set are used here to estimate the quantitative P-T conditions. Estimation of peak metamorphic P-T conditions in high-temperature granulites is often hampered by the retrograde reactions and resultant compositional changes of mineral phases (Harley, 1998,1989; Fitzsimons and Harley, 1994). When intracrystalline cation diffusion (volume diffusion) near the metamorphic peak is enough to obliterate growth zoning during prograde metamorphism, compositional equilibration among minerals occurs at peak temperature (e.g., Okudaira, 1996). After the peak conditions, the composition at the rim of the mineral phases changes along with changing P-T

conditions. Furthermore, volume diffusion within the minerals may change and obliterate the peak composition during the retrograde stage. Hence, the rim composition represents the final metamorphic re-equilibration and the core composition may indicate the near peak conditions. So, if volume diffusion within the minerals at retrograde stage is sufficient to modify composition, the true metamorphic peak temperature would be higher than that estimated by cation exchange thermometry.

Using garnet-cordierite thermometer, core compositions of the minerals yield the temperatures of 960℃ (Thompson, 1976), 860℃ (Bhattacharya et al., 1988) and 882℃ (Wells, 1979). For these temperature estimates, reference pressure is assumed to be 7 kbar. The temperature calculated using garnet-cordierite thermometers is in good agreement with the computations from spinel-cordierite Fe-Mg exchange thermometer by Vielzeuf (1983). The upper limit of temperature calculated for the core values of cordierite-spinel intergrowths is 920℃ at a reference pressure of 7 kbar. For the rim compositions of garnet and cordierite, the calculated temperatures are 770℃ (Thompson, 1976), 740℃ (Holdaway and Lee, 1977), 720℃ (Wells, 1979), 670℃ (Perchuk et al., 1985) and 760℃ (Bhattacharya et al., 1988), for the reference pressure of 4 kbar.

Metamorphic pressure conditions were estimated using the assemblage garnet-plagioclase-sillimanite-quartz. Based on the core compositions of plagioclase and garnet, the pressure estimates for the reference temperature of 900℃ is estimated to be 7.2 kbar and 7.6 kbar by using the barometers of Koziol and Newton (1988) and Koziol (1989), respectively. Based on the rim composition of garnet and plagioclase, the pressures are calculated to be 5.9 kbar (Koziol and Newton, 1988) and 6.1 kbar (Koziol, 1989). The results of the thermobarometry are illustrated in Fig. 7.
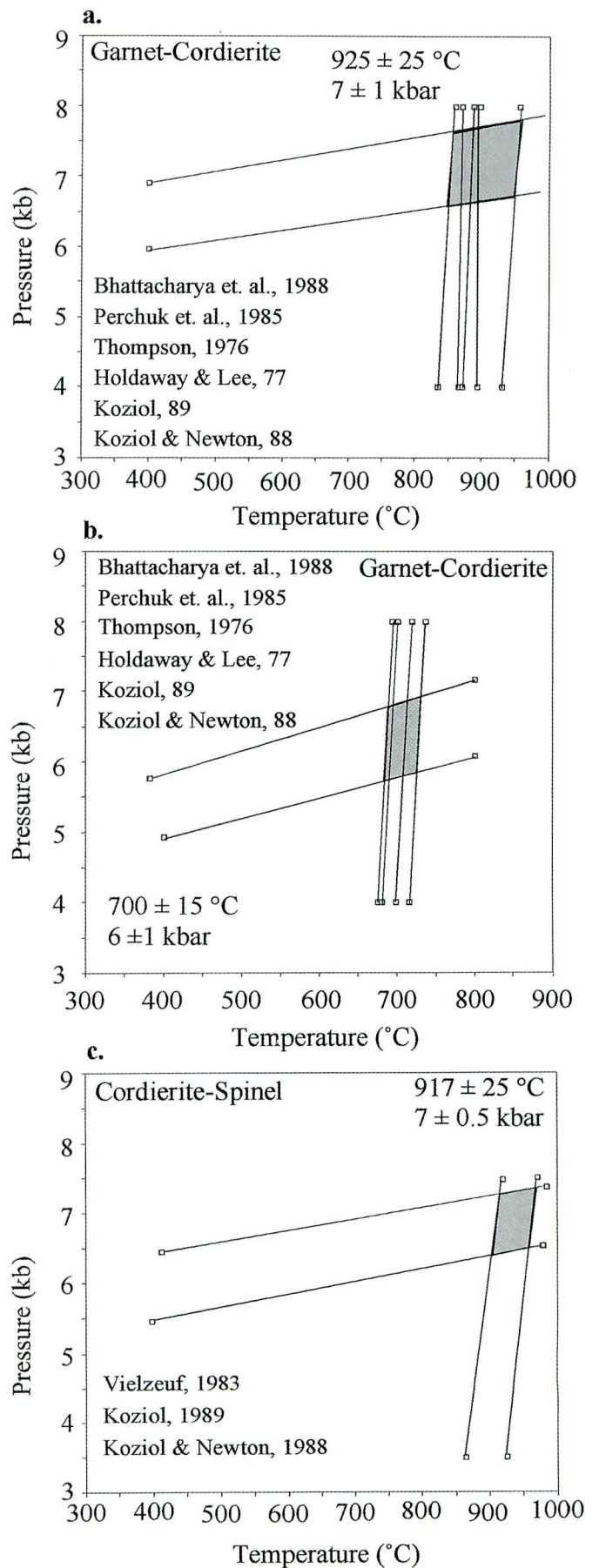
Fig. 7   (a) P-T estimates based on core compositions of garnet and cordierite, (the shaded portions in all the isopleths indicates the best-fit estimates for the equilibration P-T conditions, which may not necessarily correspond to the peak condition), (b) P-T estimation based on the rim composition of garnet and cordierite, and (c) the estimates using spinel-cordierite thermometry.

7. Discussion

7.1. Metamorphic P-T Path

The petrogenitic grid for Mg-Al rich metapelites containing K-feldspar, sillimanite and melt assemblages provides a useful base for the spinel-bearing granulites of the central KKB. The mineral assemblages of the studied samples reflect reaction around the [OPX] invariant point (Fig. 6). The results of geothermobarometry based on co-existing mineral phases suggesting peak P-T conditions of 7 kbar and ca. 930℃ are roughly consistent with the semi-quantitative considerations based on the petrogenetic grid of Fitzsimons (1996).

The observed assemblage is interpreted to have evolved from the spinel-cordierite-K-feldspar-melt (reaction1) and through the spinel-cordierite-quartz intergrowth assemblage (reaction2), which is consistent with a clockwise path through this P-T grid. Reaction (1) explained in the grid is an example for prograde reactions prior to the metamorphic peak. The decompression reaction might have occurred just after the peak metamorphism. We are thus able to document the near peak P-T path (Fig. 8) far more convincingly than previous works, which document only the retrograde path. The post peak P-T path obtained in this study for gran-

ulites from central KKB is closely comparable to the P-T path defined in other studies from KKB. Although direct evidence for ultrahigh-temperature metamorphism (>1000℃) is not preserved in these rocks, the prograde reaction textures and the high temperatures recorded from the present assemblages indicate initial melting conditions followed by decompression. The occurrence of migmatitic gneisses and garnet-bearing leucogneisses are evidence for melting reactions.
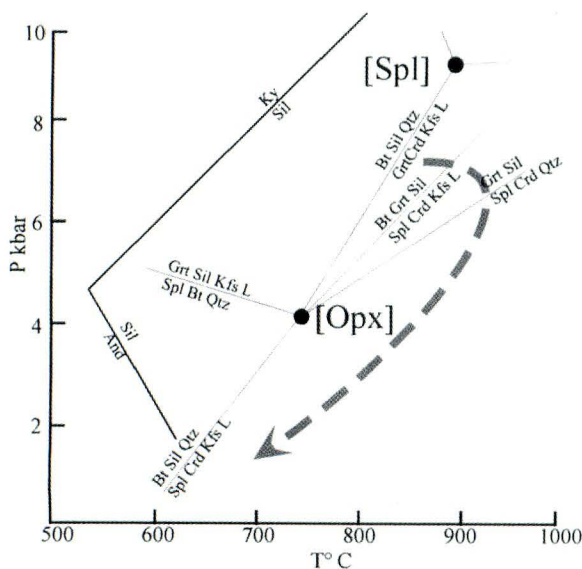
It is pertinent at this stage to compare and contrast the P-T trajectory deduced in this study with those recorded from the same terrain by previous workers. The majority of published petrological studies are from the eastern and southern part of KKB. The metamorphic peak conditions estimated in previous studies (Santosh, 1986; Chako et al., 1987) placed the peak temperatures at around 750℃. Subsequent works by Chacko et al. (1996) and Nandakumar and Harley (2000) reported further higher temperature for KKB using updates on thermobarometric calculations. Satish-Kumar and Harley (1998) reported peak temperatures of 900 ± 20℃ at pressure of 6.5-7 kbar based on mineral phase equilibria in calc-silicate rocks interlayered with the pelitic and semi-pelitic lithologies, and were suggested for the rocks from the northeastern and southern extremities. For the retrograde path, Santosh (1986) suggested an isothermal decompression (ITD) path while Chacko et al. (1987) proposed near isobaric heating followed by short isothermal decompression and an isobaric cooling profile. Santosh (1987) inferred ITD from 8kbar through to 5.5 kbar at ca. 780℃, followed by cooling to < 700℃ at a pressure of > 4 kbar. Chacko et al. (1987) did not recognize any P-T conditions > 6.5 kbar and 775℃ and suggested ITD at >750℃ to pressure down to 3 kbar. Nandakumar and Harley (2000) proposed post-peak conditions of 700-750℃ with decompression to ca. 3-4 kbar for the central KKB. Previous studies proposed relatively lower P-T conditions of granulites in central KKB as compared to those in the eastern and southern parts. Most of the studies document only near isothermal decompression and an isobaric cooling arm, and tentatively placed the former earlier than the latter. They, however, presented textural evidence only for the ITD subsequent to peak metamorphism. In our study, we demonstrate an early segment comprising some combination of heating event and decompression followed by an evolution dominated by cooling for the central KKB metapelites.

Fig. 8   The calculated P-T path for the central KKB metapelites. The two reactions meeting at [Opx] are reacton (1) and (2) which are mentioned in the text. The heavy broken line in the P-T space represents the prograde P-T path inferred from the present study.

7.2. Two-Generation Spinels

Some workers have illustrated zinc-rich spinel in

high-grade metamorphic rocks as a product of breakdown of staurolite. But in such cases, the host rocks show unusually high Zn content. In contrast, most of the minerals in the present rocks carry only negligible zinc, and the only phase other than spinel, which shows minor Zn, is biotite. Also, staurolite is totally absent in the present rocks as well as in other parts of KKB. The textural features and chemical characteristics of spinels from the central KKB metapelites suggest two generations of spinel formation during the metamorphic evolution of these rocks. The breakdown of the assemblage biotite + garnet + sillimanite resulted in the formation of brownish spinels. The gradual decrease in the zinc and chromium contents of biotite with increasing proximity to the brown spinel (Fig. 9) in the present samples suggest that these elements may be released from biotite before the complete breakdown of the mineral. This possibly occurs when the zinc saturation limit of biotite is overstepped during the pressure decrease (Dietvorst, 1980). It is suggested that the gradual decrease of the biotite zinc content with increasing proximity to spinel represents such an overstepping in the present rocks. It may be inferred from the Fig. 9 that zinc has migrated through rock during decompression over distance of at least one millimeter. The enrichment of Zn noticed in the rim portion of spinel supports this inference. The cationic exchange of Cr and Al also took place between biotite and spinel during the reaction process. Therefore it is inferred that, before the peak metamorphism, zinc bearing biotite breakdowns to form zinc-bearing spinel in the proximity of biotite.
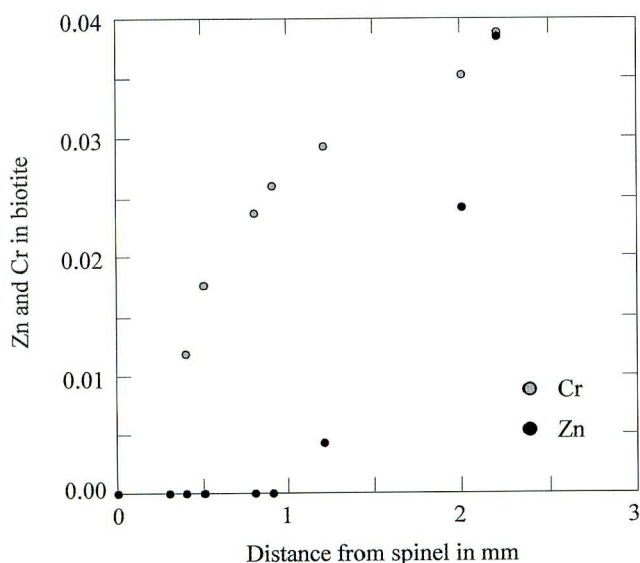
The relative decrease of Zn and Cr content in biotites to increasing distance from grain boundary of spinel lends support to this model. The brownish appearance of the later formed spinel from addition of Cr_2O_3 derived from biotites also strengthens the proposal of spinel formation by biotite breakdown.

The second category of the spinels in the study area belongs to the later stage of metamorphic evolution. As previously discussed, these later generation greenish spinels in association with secondary cordierite and quartz is formed by the breakdown of garnet + sillimanite. This variety is interpreted to have formed just after the peak and mark the equilibration of the abundant spinel-cordierite stable assemblage of the central KKB metapelites. Green colored spinel in some of the domains exists very close to quartz grains separated by a thin lamella of cordierite, thus representing their simultaneous generation. The cordierite lamella might have resulted by the breakdown of spinel + quartz. Holdaway and Lee (1977) proposed that the zinc bearing hercynite + quartz is stable at temperatures above 750°C.

8. Concluding Remarks

We obtain the following conclusions, based on the petrological analyses for the high-grade metapelites from the central KKB:
1. The petrogenetic grid considerations and computations of geothermobarometry based on co-existing mineral phases suggest P-T conditions around ~ 900°C at 7 kbar for the peak metamorphism in central KKB.
2. The inferred reaction sequence implies a prograde P-T evolution at a pressure above the [Opx] invariant point.
3. The present study also points that the breakdown of zinc-bearing biotite is considered to be able to generate spinels owing to an overstepping of the zinc saturation limit of biotite during decreasing pressure and increasing temperatures along the clockwise P-T history.

Acknowledgements

Fig. 9   Plot of Zn and Cr content of biotite versus distance from spinel grain.

References

Bence, A.E. and Albee, A.L. (1968) Empirical correction factors for the electron microanalysis of silicates and oxides. *J. Geol.*, **76**, 382-403.

Bhattacharya, A., Mazumdar, A.C. and Sen, S.K. (1988) Fe-Mg mixing in cordierite: constrains from natural data and implications for cordierite-garnet geothermometry in granulites. *Amer. Mineral.*, **73**, 338-344.

Braun, I., Raith, M. and Ravindra Kumar, G.R. (1996) Dehydration-melting phenomena in leptynitic gneisses and the generation of leucogranites: a case study from the Kerala Khondalite Belt, southern India. *J. Petrol.*, **37**, 1285-1305.

Carigton, D.P. and Harley, S.L. (1995) Partial melting and phase relations in high-grade metapelites: an experimental petrogenic grid in the KFMASH system. *Contrib. Mineral. Petrol.*, **120**, 270-291.

Chacko, T., Lamb, M. and Farquhar, J. (1996) Ultra high temperature metamorphism in the Kerala Khondalite belt. In: The Achaean and Proterozoic terrains in South India within East Gondwana. M. Santosh and M. Yoshida (Eds.), *Gondwana Research Group Memoir*, **3**, 157-165.

Chacko, T., Ravindra Kumar, G.R. and Newton, R.C. (1987) Metamorphic P-T conditions of the Kerala (S. India) Khondalite belt, a granulite facies supracrustal terrain. *J. Geol.*, **95**, 343358.

Dietvorst, E.J.L. (1980) Biotite breakdown and the formation of Gahnite in metapelitic rocks from Kemiö, Southwest Finland. *Contrib. Mineral. Petrol.*, **75**, 327-337.

Fitzsimons, I.C.W. (1996) Metapelitic migmatites from Brattstrand bluffs, East Antarctica-metamorphism, melting and exhumation of the mid crust. *J. Petrol.*, **37**, 395-414.

Fitzsimons, I.C.W. and Harley, S.L. (1994) The influence of retrograde cation exchange on granulite P-T estimates and a convergence technique for the recovery of peak metamorphic conditions. *J. Petrol.*, **35**, 543576.

Fonarev, V.I., Konilov, A.N. and Santosh, M. (2000) Multistage metamorphic evolution of the Trivandrum granulite block, southern India. *Gondwana Res.*, **3**, 293-314.

Harley, S.L. (1989) The origins of granulites: a metamorphic perspective. *Geol. Mag.*, **126**, 215247.

Harley, S.L. (1998) On the occurrence and characterisation of ultrahigh-temperature (UHT) crustal metamorphism. In: Treloar, P. J., and O'Brien, P., eds. What controls metamorphism and metamorphic reactions? *Geol. Soc. Lond. Spec. Publ.*, **138**, 75101.

Harley, S.L., Hensen, B.J. and Sheraton, J.W. (1990) Two-stage decompression in orthopyroxene-sillimanite granulites from Forefinger point, Enderby Land, Antarctica: implications for the evolution of the Archean Napier Complex. *J. Metamorph. Geol.*, **8**, 591-613.

Harris, N.B.W., Santosh, M. and Taylor, P.N. (1994) Crustal evolution in south India: contraintsts from Nd isotope. *Contrib. Mineral. Petrol.*, **102**, 139-150.

Hensen, B.J. (1987) P-T grids for silica-undersaturated granulites in the systems MAS (n+4) and FMAS (n+3) − tools for the derevation of the P-T paths of metamorphism. *J. Metmorph. Geol.*, **5**, 255-271.

Hensen, B.J. and Osanai, Y. (1994) Experimental study of dehydration melting of F-bearing biotite in model pelitic compositions. *Mineral. Mag.*, **58a**, 410-411.

Holdaway, M.J. and Lee, S.M. (1977) Fe-Mg cordierite stability in high-grade pelitic rocks based on experimental, theoretical, and natural observations. *Contrib. Mineral. Petrol.*, **63**, 175-198.

Koziol, A.M. (1989) Redetermination of the garnet-plagioclase-Al2SiO5-quartz (GASP) geobarometer and applications to natural parageneses. *EOS*, **70**, 493.

Koziol, A.M. and Newton, R.C. (1988) Redetermination of the anorthite breakdown reaction and improvement of the plagioclase-garnet-Al2SiO5-quartz barometer. *American Mineral.* **73**, 216-223.

Loomis, T.P.(1972) Contact metamorphism of pelitic rock by the Ronda ultramafic inclusion, southern Spain. *Geol. Soc. Amer. Bull.*, **83**, 433-462.

Nandakumar, V. and Harley, S.L. (2000) A reappraisal of the pressure-temperature path of granulites from the Kerala Khondalite belt, southern India. *J. Geol.*, **108**, 687-703.

Okudaira, T. (1996) Temperature-time path for the low-pressure Ryoke metamorphism, Japan, based on chemical zoning in garnet. *J. Metamorph. Geol.*, **14**, 427-440.

Perchuk, L.L., Aranovich, L.Y., Poleskii, K.K., Lavrent'eva, I.V., Gerasimove, V.Y., Fed'Kin, V.V., Kitsul, V.I., Karasakov, L.P. and Berdnikov, N.V. (1985) Precambrian granulites of Aldan shield, eastern Siberia, USSR. *J. Metamorph. Geol.*, 3, 265-310.

Plimer, I.R. (1977) The mineralogy of the high grade metamorphic rocks enclosing the Broken Hill ore bodies, Australia. *Neues. Jahrb. Mineral.*, **131**, 115-139.

Raith, M., Hoernes, S., Klatt, E. and Stahle, H.J. (1989) Contrasting mechanisms of charnockite formation in the amphibolite to granulite grade transition zones of southern India. In: Bridgwater, D., (Ed.), Fluid movements, element transport, and the composition of the deep crust: NATO ASI, **C-281**, 29-38.

Ravindra Kumar, G.R. and Chacko, T. (1986) Mechanisms of charnockite formation and breakdown in southern Kerala: implications for the origin of southern Indian granulite terrain. *J. Geol. Soc. India*, **28**, 277-288.

Robinson, P. and Jaffe, H.W. (1969) Chemographic exploration of amphebole assemblages from central Mussachusetts and southwestern New Hamshire. Mineral. Soc. *Amer. Spl. Paper*, **2**, 251-274.

Rumble, D.III. (1976) Oxide minerals in metamorphic rocks. In: Rumble, D.III., (Ed.), Oxide minerals. *Mineral Soc. Amer. Washington D.C. (short course notes)*, 3, R1-R24.

Santosh, M. (1986) Nature and evolution of metamorphic fluids in the Precambrian khondalites of Kerala, South India. *Precamb. Res.*, **33**, 283-302.

Santosh. M. (1987) Cordierite gneisses of southern Kerala, India: petrology, fluid inclusions and implications for crustal uplift history. *Contrib. Mineral. Petrol.*, **96**, 343-356.

Santosh, M. (1996) The Trivandrum and Nagercoil granulite blocks. In: The Archaean and Proterozoic terrains of southern India within East Gondwana. *Gondwana Res. Group Memoir No. 4, Field Sci. Pub.*, Osaka, 243-277.

Santosh, M., Harris, N.B.W., Jackson, D.H. and Mattey, D.P. (1990) Dehydration and incipient charnockite formation: a phase equilibria and fluid inclusion study from South India. *J. Geol.*, **98**, 915926.

Satish-Kumar, M. and Harley, S.L. (1998) Reaction textures in scapolite-wollastonite-grossular calc-silicate rock from the Kerala Khondalite Belt, southern India: evidence for high temperature and initial cooling. *Lithos*, **44**, 83-99.

Shabeer, K.P., Okudaira, T., Santosh, M. and Hayasaka, Y. (2001) First report of scheelite mineralization within granulite facies supracrustals of kerala khondalite belt, southern India. *Gondwana Res., (Abstr.vol)*, **4**, 780-783.

Srikantappa, C., Raith, M. and Speiring, B. (1985) Progressive charnockitization of a leptynite-khondalite suite in southern Kerala, India: evidence for formation of charnockites through decrease in fluid pressure?. *J. Geol. Soc. India*, **26**, 849-872.

Stoddard, E.F. (1979) Zinc rich hercynite in high grade metamorphic rocks: a product of dehydration of staurolite. *Amer. Mineral.*, **64**, 736-741.

Thompson, A.B. (1976) Mineral reactions in pelitic rocks: II. Calculation of some P-T-X (Fe-Mg) phase relations. *Amer. J. Sci.*, **276**, 425-454.

Vielzeuf, D. (1983) The spinel and quartz association in high grade Xenoliths from Tallante (S.E. Spain) and their potential use in geothermometry and barometry. *Contrib. Mineral. Petrol.*, **82**, 301-311.

Wall, V.J. and England, R.N. (1979) Zn-Fe spinel-silicate-sulphide reactions as sensors of metamorphic intensive variables and processes. *Geol. Soc. Amer., (Abstr.)*, **11**, 534.

Wells, P.R.A. (1979) Chemical and thermal evolution of Archean sialic crust, southern West Greenland: *J. Petrol.*, **20**, 187-266.